States built on the 10^{+} isomers in ^{118,120,122,124}Sn

N. Fotiades, M. Devlin, R. O. Nelson, J. A. Cizewski, R. Krücken, R. M. Clark, P. Fallon, I. Y. Lee, A. O. Macchiavelli, and W. Younes

Phys. Rev. C **84**, 054310 — Published 16 November 2011
DOI: 10.1103/PhysRevC.84.054310

States built on the 10^+ isomers in ^{118,120,122,124}Sn

N. Fotiades,* M. Devlin, and R. O. Nelson
Los Alamos National Laboratory, Los Alamos, New Mexico 87545, USA

J. A. Cizewski
Department of Physics and Astronomy, Rutgers University, New Brunswick, New Jersey 08903, USA

R. Krücken
Physik Department E12, Technische Universität München, D-85748 Garching, Germany; TRIUMF, Vancouver, V6T 2A3, Canada

R. M. Clark, P. Fallon, I. Y. Lee, and A. O. Macchiavelli
Nuclear Science Division, Lawrence Berkeley National Laboratory, Berkeley, California 94720, USA

W. Younes
Lawrence Livermore National Laboratory, Livermore, California 94550, USA
(Dated: October 24, 2011)

The high-spin structure above the previously known 10^+ isomers of the ^{118,120,122,124}Sn isotopes was studied via prompt γ-ray spectroscopy. All isotopes were populated as fragments following the fission of much heavier compound nuclei formed in three fusion-fission reactions. ^{118,120,122}Sn were also independently populated and studied as evaporation residues in the ^{124}Sn$(n, xn\gamma)$ reactions, with $x = 3, 5, 7$. Transitions above the previously known 10^+ isomers were observed for the first time and the corresponding level schemes above these isomers were established up to 6646-, 5673-, 5386-, and 5952-keV excitation energy for ^{118,120,122,124}Sn, respectively. The experimental results are compared with predictions from shell-model calculations.

PACS numbers: PACS number(s): 23.20.Lv, 27.60.+j, 25.40.-h, 28.20.-v

I. INTRODUCTION

The tin isotopic chain, with thirty one semi-magic isotopes between the two double-magic isotopes of ^{100}Sn and ^{132}Sn, has been a testing ground for models and methods in nuclear structure for many decades [1, 2]. Along this chain the collectivity is expected to be highest around mid-shell, i.e. in ^{116}Sn. However, recent expanded shell model calculations indicate a slightly shifted shallow maximum in the transition probability values around ^{118,120}Sn [3], closer to recent experimental findings [2], and attributed to the inhibiting effect that the $s_{1/2}$ orbital has on collectivity, when located near the Fermi level in this region [2]. The study of high-spin states in ^{118,120,122,124}Sn merits additional attention since these isotopes are located near the middle of the shell that spans the tin isotopic chain.

The level schemes of the Sn isotopes include mostly neutron excitations across the subshells between the shell gaps at $N = 50$ and $N = 82$ because of the closed proton shell at $Z = 50$. For $N > 64$ these include single-particle and hole excitations in the $h_{11/2}$ neutron orbital, as well as in the close-lying $d_{3/2}$ and $s_{1/2}$ orbitals. The short-range repulsive character of the nucleon-nucleon interaction leads to a small level spacing between the highest-spin levels of multiplets, where the wave functions do not reach maximum overlap due to the Pauli principle, producing several isomeric states. Candidates for the 10^+ isomeric states are known in all even-mass Sn isotopes in the $A = 122$ mass region, as summarized in Refs. [4, 5], and a (15^-), 220(30) ns isomer was observed in ^{128}Sn recently [6]. Lower spin, 7^- and 5^- isomers have also been identified.

In ^{118,120,122,124}Sn isomers have been previously observed at 3108-, 2902-, 2766-, and 2657-keV excitation energy, and with 2.5-, 6.26-, 62-, and 45-μs half lives [7–11], respectively. The 10^+ spin-parity assignments of these isomers remain tentative, except perhaps in the case of ^{118}Sn where the most recent published level scheme in Ref. [8] includes the 10^+ spin-parity assignment without parentheses. Nothing was known about the structure above these isomers before the present work. (10^+) isomers are also known in the heavier even-mass Sn isotopes [4, 5] with limited spectroscopic information available above the (10^+) isomer only in the case of ^{128}Sn [6]. The lack of information on

*fotia@lanl.gov

high-spin states above the isomers in these isotopes is mainly due to their μs half-lives and to the increasing lack with increasing mass number of suitable stable beam-target combinations to populate high-spin states in these isotopes as evaporation residues in heavy-ion fusion reactions. High-spin states in the off-yrast intruder deformed band of ^{118}Sn, whose deexcitation by-passes the known isomers in this isotope, have been recently reported [8].

An alternative way to study high-spin states in ^{118,120,122,124}Sn would be the prompt γ-ray spectroscopy of fission fragments in fusion-fission reactions of much heavier nuclei. Such methods have been used several times to collect information on high-spin states of stable nuclei or nuclei near the line of stability (see, for instance, Ref. [12]). ^{118,120,122,124}Sn can be populated as fission fragments in such reactions and the structure above their isomers can be studied by establishing γ-ray coincidences between transitions feeding the isomers and previously known transitions in the complementary fission fragments. This method was used here together with the population of ^{118,120,122}Sn in (n, xn) reactions on stable ^{124}Sn. The same approach was also applied in studying high-spin states above the $11/2^-$ isomer in ^{135}Xe [13] populated in the $(n, 2n)$ evaporation channel and as a fission fragment. The ^{124}Sn(n, n') reaction channel only populated states below $10\hbar$ in ^{124}Sn with sufficient intensity to be experimentally observed.

II. EXPERIMENTS

The beam for the three fusion-fission experiments, henceforth referred to as Experiments I, II and III, in this work was provided by the 88-Inch Cyclotron Facility at Lawrence Berkeley National Laboratory. The Gammasphere array was used to detect "prompt"-time coincidences between γ rays in all cases with the width of the time overlap allowed between coincidences in the data acquisition trigger being $\sim$100 ns. In Experiment I, Gammasphere comprised 92 Compton-suppressed large volume HPGe detectors, while in Experiments II and III the number of Ge detectors was 100.

In Experiment I a ^{197}Pb compound nucleus (CN) was formed in the ^{24}Mg + ^{173}Yb reaction at 134.5 MeV. The target consisted of 1 mg/cm^2 isotopically enriched ^{173}Yb, evaporated on a 7 mg/cm^2 gold backing (reactions of the beam in the backing produce a ^{221}Pa CN). In Experiment II a ^{199}Tl CN was formed in the ^{23}Na + ^{176}Yb reaction at a beam energy of 129 MeV. The target consisted of approximately 1 mg/cm^2 isotopically enriched ^{176}Yb on a 10 mg/cm^2 Au backing (reactions of the beam in the backing produce a ^{220}Th CN). In Experiment III a ^{226}Th compound nucleus was populated in the ^{18}O + ^{208}Pb reaction at 91 MeV and the target was 45 mg/cm^2 in areal density. About 2.3$\times10^9$ triples, 10^9 quadruples, and 2.5$\times10^9$ quadruples, were collected in Experiments I, II and III, respectively. Symmetrized, three-dimensional cubes were constructed to investigate the coincidence relationships between the γ rays. Additional information for Experiments I, II and III can be found in Refs. [14–16].

The ^{124}Sn(n, xn) measurement described in this work, henceforth referred to as Experiment IV, was performed at the Los Alamos Neutron Science Center Weapons Neutron Research (LANSCE/WNR) facility [17]. The γ rays were produced in the bombardment by neutrons of a 1 g ^{124}Sn foil, 97.9% isotopically enriched and $\sim$0.1 cm thick, and were observed with the GEANIE spectrometer [18, 19]. GEANIE is located 20.34 m from the WNR spallation neutron source on the 60R (60°-Right) flight path. The neutrons were produced in a $^{\rm nat}$W spallation target driven by an 800-MeV proton beam. The beam time structure in the present experiment consisted of 590 μs-long "macropulses", with each macropulse containing subnanosecond-wide "micropulses", spaced every 1.8 μs. The energy of the neutrons was determined using the time-of-flight technique. GEANIE is comprised of 11 Compton-suppressed planar Ge detectors (low-energy photon spectrometers - LEPS), 9 Compton-suppressed coaxial Ge detectors and 6 unsuppressed coaxial Ge detectors. A total of $\sim 6 \times 10^8$ γ singles and higher-fold data were recorded.

III. EXPERIMENTAL RESULTS

Partial level schemes of ^{118,120,122,124}Sn as obtained in the present work are shown in Fig. 1. All transitions and levels above the (10^+) isomers in Fig. 1 are observed for the first time. A summary of all other previously-known states and transitions of ^{118}Sn is given in Ref. [7], where the spin-parity assignment of the 3108-keV isomer is quoted as 9^+,10^+. The level scheme of ^{118}Sn was recently enriched with the results in Ref. [8], where a firm 10^+ spin-parity assignment for the isomer is proposed. Thus, 10^+ spin-parity assignment for this isomer of ^{118}Sn was adopted in Fig. 1. Summaries for ^{120,122,124}Sn are given in Refs. [9–11]. The placement of the transitions in Fig. 1 is based on their established coincidence relationships in Experiments I, II and III, and on their intensity, also quoted in Fig. 1 for each transition, relative to the lowest transitions in all level schemes. For ^{118}Sn the relative intensities quoted are those from Experiment I, whereas for ^{120,122,124}Sn the quoted relative intensities were obtained in Experiment III. The assignment of the structures built on the (10^+) isomers in Fig. 1 to each isotope is based on establishing coincidences between each of the 1237.8-, 1190.1-, 1103.3-, and 1046.8-keV transitions and previously-known transitions belonging to complementary fission fragments in experiments I, II and III, as well as determining the neutron excitation functions for the 1237.8-, 1190.1-, and 1103.3-keV transitions in Experiment IV, as described below.

A. Experiments I, II and III

The compound nucleus in Experiment III (^{226}Th) is the heaviest and the most neutron rich ($N/Z = 1.51$) among the three experiments. The compound nuclei in Experiments I and II are of similar mass with those in Experiment II more neutron rich than in Experiment I. The transitions assigned to ^{118}Sn in Fig. 1 were observed in Experiments I and II with similar strength, but not observed in Experiment III. The sequence assigned to ^{120}Sn in Fig. 1 was observed in all three experiments; however, it is stronger in Experiment III. The sequence assigned to ^{122}Sn in Fig. 1 is observed strongly in Experiment III and is very weak in Experiment II. Finally, the sequence assigned to ^{124}Sn in Fig. 1 is observed in Experiment III only. These observations are in accordance with the assignment of the sequence on the left in Fig. 1 to the lightest isotope and the rest of the sequences from left to right in Fig. 1 to isotopes with increasing mass. Consequently, the spectra shown below for ^{118}Sn originate from Experiments I and II, whereas for ^{120,122,124}Sn the spectra shown originate from Experiment III.

In order to identify candidates for transitions above the (10^+) isomers, the patterns of intensities for the fragments that are complementary to ^{118,120,122,124}Sn in all three experiments were determined. In Fig. 2.a the double gate from Experiment I on the previously known 1229.7-keV, $2_1^+ \rightarrow 0_1^+$, and 1050.7-keV, $4_1^+ \rightarrow 2_1^+$, transitions of ^{118}Sn [7] is displayed; the 132.3-, 221.7-, 254.9- (lies under the stronger 253.7-keV peak), 824.7-, 978.0-, and 1641.0-keV transitions belonging to the complementary ^{95,96,97}Nb [12, 20] fragments are present in this spectrum. In Fig. 2.b, the double gate on the candidates above the 10^+ isomer, the 1237.8- and 585.5-keV transitions from Fig. 1, displays a similar intensity pattern for the same complementary fragments. All transitions assigned to ^{118}Sn in Fig. 1 can be seen in the spectrum in Fig. 2.b, except, of course, for the transitions that form the double gate. All previously-known transitions of ^{118}Sn present in Fig. 2.a are not seen in Fig. 2.b, and vice versa, suggesting that the transitions in Fig. 2.b lie above an isomer with half life much larger than the ~100 ns time-window, as is the case for the 2.5-μs isomer in ^{118}Sn. Similar spectra were obtained in Experiment II. ^{118}Sn was populated in the $6n, 7n$, and $8n$ channels in both experiments.

Spectra from Experiment III are shown in Figs. 3 and 4. The double gate on the previously known 1171.3-keV, $2_1^+ \rightarrow 0_1^+$, and 1023.0-keV, $4_1^+ \rightarrow 2_1^+$, transitions of ^{120}Sn [9] is shown in Fig. 3.a; the 212.1-, 351.6-, 411.6-, 497.6-, and 1222.7-keV transitions belonging to the complementary ^{98,99,100}Zr [21–23] fragments are present in this spectrum. The double gate on the 1190.1- and 556.4-keV transitions from Fig. 1 is shown in Fig. 3.b. Exactly the same previously-known transitions from the Zr complementary fragments and with similar intensity patterns are present in both spectra, suggesting assignment of the 1190.1- and 556.4-keV transitions to ^{120}Sn. All transitions assigned to ^{120}Sn in Fig. 1 can be seen in the spectrum in Fig. 3.b, except for the transitions that form the double gate. All previously-known transitions of ^{120}Sn present in Fig. 3.a are not seen in Fig. 3.b, and vice versa, suggesting that the transitions in Fig. 3.b lie above an isomer with half life much larger than the ~100 ns time-window, as is the case for the 6.26-μs isomer in ^{120}Sn. Transitions from the ^{98,99,100}Zr [21–23] fission fragments are observed in Fig. 3, hence, ^{120}Sn is populated in the $8n, 7n, 6n$ neutron-emitting channels, respectively. The double gates on the previously known 1140.5-keV, $2_1^+ \rightarrow 0_1^+$, and 1001.5-keV, $4_1^+ \rightarrow 2_1^+$, transitions of ^{122}Sn [10], and on the 1103.3- and 1030.3-keV transitions in Fig. 1 are shown in Fig. 4.a and 4.b, and exhibit similar intensity patterns for the corresponding ^{96,97,98,100}Zr [21, 24–26] fragments. In Fig. 4.c the double gate on the previously known 1131.7-keV, $2_1^+ \rightarrow 0_1^+$, and 970.0-keV, $4_1^+ \rightarrow 2_1^+$, transitions of ^{124}Sn [11] is shown. The ^{98}Zr [21] 1222.7-keV, $2_1^+ \rightarrow 0_1^+$ transition is the strongest with significant population of ^{96}Zr [24] (1750.4-keV, $2_1^+ \rightarrow 0_1^+$ transition) and presence of weaker transitions from the odd-mass ^{95,97}Zr [24, 25, 27] complementary fragments. In Fig. 4.d, the double gate on the candidate transitions above the (10^+) isomer in ^{124}Sn, the 1046.8- and 995.8-keV transitions from Fig. 1, displays a similar intensity pattern for the corresponding fragments.

The actual sequence of identification of the Sn 556.4-, 585.5-, 995.8-, 1030.3-, 1046.8-, 1103.3-, 1190.1-, and 1237.8-keV transitions during the analysis of the data in Experiments I, II and III is the following. First, the 1046.8-, 1103.3-, 1190.1- and 1237.8-keV transitions were observed in double gates on previously-known transitions of complementary fission fragments (see, for example, Fig. 5). Then the 556.4-, 585.5-, 995.8-, and 1030.3-keV transitions were identified in double gates between the 1046.8-, 1103.3-, 1190.1- or 1237.8-keV transitions and previously-known transitions of complementary fission fragments. Last, the coincidence relationship of the transitions was established together with the rest of the partial level schemes in Fig. 1.

In Experiment III only one compound nucleus (^{226}Th) is formed; hence, the assignment of the transitions to a tin isotope, after their observation in the Zr gates is unique and straightforward. On the contrary, in Experiments I and II, reactions of the beam with the targets form the ^{197}Pb and ^{199}Tl CN, respectively, and reactions of the beam in the backing form the compound nuclei ^{221}Pa and ^{220}Th, respectively. Potential assignment of the 1237.8- and 585.5-keV transitions to a niobium isotope, which would be the complementary fragment with respect to the ^{197}Pb and ^{199}Tl CN, can be safely ruled out. For a specific Nb isotope the neutron-emitting channels would be different in the two reactions, e.g., if ^{97}Nb [12] is the complementary fragment, that would imply $8n, 7n, 6n$ neutron-emitting channels in Experiment II (^{199}Tl CN), with respect to the ^{94,95,96}Zr complementary fragments, and only $6n, 5n, 4n$ neutron-emitting channels in Experiment I (^{197}Pb CN), with respect to the ^{95,96,97}Nb complementary fragments. However, seeing at most 6 neutrons is lower than the usual number of neutrons observed in both reactions. In addition, and most important, the neutron excitation function for the 1237.8-keV transition was obtained in Experiment IV and supports independently the assignment of the transition to a tin isotope, as discussed below.

B. Experiment IV

The assignment of the 1103.3-, 1190.1- and 1237.8-keV transitions to ^{122}Sn, ^{120}Sn, and ^{118}Sn, respectively, was deduced independently in the (n, xn) experiment, where the excitation functions for these transitions were obtained versus incident neutron energy. Examples of typical excitation functions obtained for previously known transitions of $^{117-123}$Sn [7, 9, 10, 28–31] in Experiment IV are shown in Figs. 6, 7 and 8. As shown in Fig. 6, a typical excitation function for a transition of ^{123}Sn [the $(n, 2n)$ reaction channel] peaks at incident neutron energies between 10- and 20-MeV, that of ^{122}Sn [the $(n, 3n)$ reaction channel] peaks at higher incident neutron energies (between 20- and 30-MeV) due to the additional incident neutron energy that is required for emission of the third neutron, and so on. The excitation function for the 1103.3-keV transition is shown in Fig. 6 and exhibits the typical characteristics of a transition in the ^{124}Sn$(n, 3n)$ reaction channel. Namely, it peaks between 20- and 30-MeV neutron energies, has a higher neutron energy threshold than the excitation function of the 1140.5-keV, $2^+ \rightarrow 0^+$ transition of ^{122}Sn, and peaks at a lower neutron energy from the excitation function of the transition from the immediately higher neutron channel (1151-keV, $(15/2^-) \rightarrow 11/2^-$ transition of ^{121}Sn, the $(n, 4n)$ reaction channel). Hence, the characteristics of the excitation function for the 1103.3-keV transition in Fig. 6 confirm its assignment to ^{122}Sn. All other transitions in Fig. 1 above the 1103.3-keV transition are much weaker; most likely they are emitted from higher-spin states, and were not observed in Experiment IV. Similarly, in Fig. 7, a typical excitation function for a transition of ^{120}Sn [the $(n, 5n)$ reaction channel] peaks at neutron energies between 40- and 50-MeV, and the excitation function for the 1190.1-keV transition exhibits the typical characteristics of such a transition confirming the assignment to ^{120}Sn. In order to keep the same time resolution in the time-of-flight technique used in Experiment IV, the neutron-energy bins become wider at higher neutron energies, as can be seen from comparison of Figs. 6, 7, and 8. Hence, the neutron energy resolution becomes worse with increasing neutron energy in these figures. The excitation function for the 1229.7-keV, $2_1^+ \rightarrow 0_1^+$ transition of ^{118}Sn in Fig. 8, peaks at $\sim$70 MeV neutron energy whereas that for the 1278.2-keV, $15/2_1^- \rightarrow 11/2_1^-$ transition of ^{117}Sn peaks at $E_n \sim$90 MeV. The excitation function for the 1237.8-keV transition lies in between these two excitation functions, suggesting origin from the $(n, 7n)$ reaction channel, i.e., assignment to ^{118}Sn. A similar excitation function, but with larger errors due to poor statistics, was obtained also for the 585.5-keV transition.

The absolute partial cross sections for the production of transitions observed in Experiment IV will be the subject of a future article. In the present work only the neutron excitation functions established for these transitions are important. The cross sections were used here only in determining the intensity of the transitions relative to the $2^+ \rightarrow 0^+$ transitions in ^{118,120,122}Sn. Specifically, the intensities of the 585.5- and 1237.8-keV transitions relative to that of the 1229.7-keV transition in ^{118}Sn are $\sim$6% and $\sim$20%, respectively; the intensity of the 1190.1-keV transition relative to that of the 1171.3-keV transition in ^{120}Sn is $\sim$10%; and a $\sim$0.7% intensity was determined for the 1103.3-keV transition relative to the intensity of the 1140.5-keV, $2^+ \rightarrow 0^+$ transition of ^{122}Sn. In all cases the quoted relative intensity was corrected for γ-ray efficiency and for γ-ray attenuation inside the target. Since the energies of these pairs of transitions are very close to each other, these corrections were insignificant, except in the case of the 585.5- and 1229.7-keV transition pair. The relative intensity of the transitions depend strongly on the neutron energy. Hence, at a given neutron energy the relative intensities can be different from those reported here which are average relative intensities over all neutron energy bins. A stronger population of higher-spin states is established with increasing x in the ^{124}Sn(n, xn) reaction, as is expected from the higher neutron energies that are required to open channels with more emitted neutrons. This explains the lack of observation of the 1046.8-keV transition in Experiment IV. This transition is assigned to ^{124}Sn and would be populated in the ^{124}Sn(n, n') reaction channel (typical excitation functions for transitions in this channel peak at neutron energies below 10 MeV) with an expected relative intensity (by extrapolation of the relative intensity numbers above) of less than $\sim$0.1%, which lies below the observation limit in Experiment IV.

Spin and parity assignments of all levels reported in this work are difficult to deduce experimentally due to the lack of directional correlation information for the fission products in Experiments I, II, and III, and insufficient statistics in Experiment IV. The only experimental conclusion is that the 3869-keV level of ^{122}Sn and the 4092-keV level of ^{120}Sn in Fig. 1 are likely high-spin states since the excitation functions for the 1103.3- and 1190.1-keV transitions in Figs. 6 and 7 peak at a higher neutron energy and have a higher neutron-energy threshold compared to the excitation functions of the 1140.5- and 1171.3-keV, $2_1^+ \rightarrow 0_1^+$ transitions of ^{122}Sn and ^{120}Sn, respectively. Although in Experiment IV the energy resolution becomes worse with increasing neutron energy, in Fig. 8 the neutron excitation function of the 1237.8-keV transition compared to that of the 1229.7-keV, $2_1^+ \rightarrow 0_1^+$ transition of ^{118}Sn, supports a high-spin assignment to the 4346-keV level of ^{118}Sn.

IV. DISCUSSION

The low-lying states of Sn isotopes are predominantly formed by neutron excitations corresponding to spherical configurations. Above $N > 64$, where the neutron $d_{5/2}$ and $g_{7/2}$ orbitals are filled, isomers with 5^- and 7^- spin-parities, attributed to the neutron $h_{11/2}s_{1/2}$ and $h_{11/2}d_{3/2}$ configurations, respectively, are important in the moderate spin part of the level schemes. At higher spins, (10^+) isomers have been observed in the $^{116-130}$Sn isotopes [4, 5, 7–11, 32–35] with a maximum half-life at ^{122}Sn due to the half-filled $h_{11/2}$ neutron orbital. The 10_1^+ states may be interpreted to arise from the neutron $h_{11/2}^2$ configuration and their excitation energy drops smoothly with mass number. They have been studied with various methods including deep inelastic reactions on Sn isotopes [36, 37], light-ion reactions on Cd isotopes [38], as well as the β-decay of In isotopes [39]. In Fig. 9 the systematics of the (10_1^+) and (12_1^+) states in the even-mass $^{116-130}$Sn isotopes [6–11, 32–35] are summarized. The (12_1^+) states are seen to behave smoothly with mass number following the lower (10_1^+) states.

In the shell model calculations in Ref. [40] a pair of 11^+ and 12^+ states are predicted above the 10_1^+ isomers in all even-mass tin isotopes from ^{114}Sn to ^{128}Sn with excitation energies that decrease smoothly with mass number. In these isotopes the 11^+ and 12^+ states have the same structure, namely $2_1^+ \otimes 10_1^+$, the difference in their excitation energy is very small, and the 11^+ state is predicted to become off-yrast for ^{120}Sn and heavier tin isotopes. The rest of the members of the $2_1^+ \otimes 10_1^+$ multiplet are expected to be at high excitation energies and are off-yrast states. Indeed, the 11^+ and 12^+ states in neighboring ^{116}Sn are reported at 4702- and 4882-keV excitation energy [32], only 180 keV apart, and in excellent agreement with the shell model predictions. The energy difference between these states is predicted to become even smaller in ^{118,120,122,124}Sn. Hence, the population of the 11^+ states in the production of ^{118,120,122,124}Sn as fission fragments is expected to be very weak, with the bulk of intensity following the yrast line via the 12^+ states. The tentative 12^+ spin-parity assignments in the present work for the 4346-, 4092-, 3869-, and 3703-keV states in ^{118,120,122,124}Sn, respectively, are in excellent agreement with the shell model calculations.

In Table I the energies of the $(12_1^+) \rightarrow (10_1^+)$ transitions relative to the $2_1^+ \rightarrow 0_1^+$ transitions are summarized for the $N > 64$ even-mass Sn isotopes. The ratios of these transition energies are large ($\sim$1) suggesting collectivity similar to that of the 2^+ states. In the simplest shell model above $N = 64$, where the $d_{5/2}$ and $g_{7/2}$ neutron orbitals are filled, neutrons in the $h_{11/2}$ orbital will become more important in the wave function of the 2_1^+ state, since only $(d_{3/2})^2$ and $d_{3/2}s_{1/2}$ configurations can also contribute to 2^+ excitations. That the $12_1^+ \rightarrow 10_1^+$ transition energies are essentially identical to the $2_1^+ \rightarrow 0_1^+$ energies suggests little blocking of the quadrupole collectivity when two neutrons are aligned to form the 10_1^+ state.

The calculations of Ref. [40] predict that the wave functions of the 2_1^+ states up to ^{130}Sn are very complicated, with sizeable contributions from the $g_{7/2}$ and $d_{5/2}$ neutrons, with at most 60% (amplitude <0.8) of the wave function coming from $(h_{11/2})^2_{2^+}$ for $A > 122$. The tentative assignment of the $12_1^+ \rightarrow 10_1^+$ transition in ^{128}Sn [6] shows that probably the trend of increased collectivity above the 10^+ Sn isomers persists for $A > 124$.

V. SUMMARY

In summary, the level schemes above the previously known (10^+) isomers of ^{118,120,122,124}Sn were established up to 6646-, 5673-, 5386-, and 5952-keV excitation energy, respectively. The assignment of new transitions to ^{118,120,122,124}Sn was deduced from three experiments populating these isotopes as fragments following the fission of much heavier compound nuclei formed in fusion-fission reactions. Confirmation of the assignments came from neutron-induced reactions on ^{124}Sn populating ^{118,120,122}Sn as evaporation residues in the $(n, 7n)$, $(n, 5n)$, and $(n, 3n)$ reaction channels, respectively. The first excited states above the (10^+) isomers are most likely the (12^+) states the energies of which are seen to behave smoothly with mass number and follow the lower (10^+) systematics. Good agreement is observed between the newly identified (12^+) level energies in ^{118,120,122,124}Sn and those predicted by shell-model calculations reported previously in the literature. γ-ray energy ratios indicate collectivity for the 12^+ states similar to that of the 2^+ states.

Acknowledgments

This work has been supported in part by the U.S. Department of Energy under Contract Nos. DE-AC52-06NA25396 (LANL), DE-AC52-07NA27344 (LLNL) and AC03-76SF00098 (LBNL), and by the National Science Foundation (Rutgers). This work has benefitted from use of the LANSCE accelerator facility supported under DOE Contract No. DE-AC52-06NA25396.

[1] A. Bohr and B. Mottelson, Nuclear structure, vol. 2 (Benjamin, New York, 1975).
[2] A. Jungclaus *et al.*, Phys. Lett. **B 695**, 110 (2011).
[3] A. Ekström *et al.*, Phys. Rev. Lett. **101**, 012502 (2008).
[4] J. J. Ressler *et al.*, Phys. Rev. C **81** 014301 (2010).
[5] R. L. Lozeva *et al.*, Phys. Rev. C **77** 064313 (2008).
[6] S. Pietri *et al.*, Phys. Rev. C **83** 044328 (2011).
[7] K. Kitao, Nucl. Data Sheets **75**, 99 (1995).
[8] S. Y. Wang *et al.*, Phys. Rev. C **81**, 017301 (2010).
[9] K. Kitao, Y, Tendow, and A. Hashizume, Nucl. Data Sheets **96**, 241 (2002).
[10] T. Tamura, Nucl. Data Sheets **108**, 455 (2007).
[11] J. Katakura and Z. D. Wu, Nucl. Data Sheets **109**, 1655 (2008).
[12] N Fotiades *et al.*, Phys. Rev. C **82** 044306 (2010).
[13] N Fotiades *et al.*, Phys. Rev. C **75** 054322 (2007).
[14] N. Fotiades *et al.*, Phys. Rev. C **67**, 034602 (2003).
[15] R. Krücken *et al.*, Eur. Phys. J. A **5**, 367 (1999).
[16] N. Fotiades *et al.*, Phys. Rev. C **74**, 034308 (2006).
[17] P. W. Lisowski, C. D. Bowman, G. J. Russell, and S. A. Wender, Nucl. Sci. Eng. **106**, 208 (1990).
[18] J. A. Becker and R. O. Nelson, Nuclear Physics News International **7**, 11 (June, 1997).
[19] N. Fotiades *et al.*, Phys. Rev. C **69**, 024601 (2004).
[20] D. Bucurescu *et al.*, Phys. Rev. C **71**, 034315 (2005).
[21] G. S. Simpson *et al.*, Phys. Rev. C **74**, 064308 (2006).
[22] C. Y. Wu *et al.*, Phys. Rev. C **70**, 064312 (2004).
[23] H. Hua *et al.*, Phys. Rev. C **69**, 014317 (2004).
[24] D. Pantelica *et al.*, Phys. Rev. C **72**, 024304 (2005).
[25] N. Nica, Nucl. Data Sheets **111**, 525 (2010).
[26] B. Singh, Nucl. Data Sheets **109**, 297 (2008).
[27] N. Fotiades *et al.*, Phys. Rev. **C 65** 044303 (2002).
[28] O. Hashimoto, Y. Shida, G. Ch. Madueme, N. Yoshikawa, M. Sakai, and S. Ohya, Nucl. Phys. **A318**, 145 (1979).
[29] D. M. Symochko, E. Browne, and J. K. Tuli, Nucl. Data Sheets **110**, 2945 (2009).
[30] S. Ohya, Nucl. Data Sheets **111**, 1619 (2010).
[31] S. Ohya, Nucl. Data Sheets **102**, 547 (2004).
[32] J. Blachot, Nucl. Data Sheets **111**, 717 (2010).
[33] J. Katakura and K. Kitao, Nucl. Data Sheets **97**, 765 (2002).
[34] M. Kanbe and K. Kitao, Nucl. Data Sheets **94**, 227 (2001).
[35] B. Singh, Nucl. Data Sheets **93**, 33 (2001).
[36] R. Broda *et al.*, Phys. Rev. Lett. **68**, 1671 (1992).
[37] R. H. Mayer *et al.*, Phys. Lett. **B336**, 308 (1994).
[38] S. Lunardi *et al.*, Z. Phys. A **328**, 487 (1987).
[39] B. Fogelberg, K. Heyde, and J. Sau, Nucl. Phys. **A352**, 157 (1981).
[40] A. Insolia, N. Sandulescu, J. Blomqvist, and R. J. Liotta, Nucl. Phys. **A550**, 34 (1992).

TABLE I: Gamma-ray energies of the $(12_1^+) \to (10_1^+)$ transitions and the $2_1^+ \to 0_1^+$ transitions, their ratios and energy differences in ^{116,118,120,122,124,128}Sn. Data from Refs. [6–11, 32] and the present work. Values in parentheses are tentative and originate from the tentative assignment of the 1061-keV transition as $(12^+) \to (10^+)$ in ^{128}Sn [6].

Isotope	$E_{\gamma 12}$ $(12_1^+ \to 10_1^+)$ (keV)	$E_{\gamma 2}$ $(2_1^+ \to 0_1^+)$ (keV)	$E_{\gamma 12}$ / $E_{\gamma 2}$	$E_{\gamma 12} - E_{\gamma 2}$ (keV)
^{116}Sn$_{66}$	1335.2	1293.5	1.032	41.7
^{118}Sn$_{68}$	1237.8	1229.7	1.007	8.1
^{120}Sn$_{70}$	1190.1	1171.3	1.016	18.8
^{122}Sn$_{72}$	1103.3	1140.5	0.967	-37.2
^{124}Sn$_{74}$	1046.8	1131.7	0.925	-84.9
^{128}Sn$_{78}$	(1061)	1169	(0.908)	(-108)

FIG. 1: Partial level schemes assigned to ^{118,120,122,124}Sn in the present work. Transition and excitation energies are given in keV. The width of the arrows is representative of the intensity of the transitions which is quoted for each transition. The intensities quoted for ^{118}Sn are from Experiment I and for ^{120,122,124}Sn are from Experiment III. The uncertainty on the γ-ray energies varies from 0.4 keV to 0.9 keV.

FIG. 2: Background subtracted spectra from Experiment I gated on (a) the previously known 1229.7-keV, $2_1^+ \rightarrow 0_1^+$, and 1050.7-keV, $4_1^+ \rightarrow 2_1^+$, transitions of ^{118}Sn [7], and (b) the 1237.8- and 585.5-keV transitions in Fig. 1. The energies of the transitions are in keV. Transitions associated with the complementary ^{95,96,97}Nb [12, 20] isotopes are indicated. Weak unlabelled peaks in both spectra are most likely contaminants.

FIG. 3: Background subtracted spectra from Experiment III gated on (a) the previously known 1171.3-keV, $2_1^+ \rightarrow 0_1^+$, and 1023.0-keV, $4_1^+ \rightarrow 2_1^+$, transitions of ^{120}Sn [9], and (b) the 1190.1- and 556.4-keV transitions in Fig. 1. The energies of the transitions are in keV. Transitions associated with the complementary ^{98,99,100}Zr [21–23] isotopes are indicated. Weak unlabelled peaks in both spectra are most likely contaminants.

FIG. 4: Background subtracted spectra from Experiment III gated on (a) the previously known 1131.7-keV, $2_1^+ \rightarrow 0_1^+$, and 970.0-keV, $4_1^+ \rightarrow 2_1^+$, transitions of ^{124}Sn [11], (b) the 1046.8- and 995.8-keV transitions in Fig. 1, (c) the previously known 1140.5-keV, $2_1^+ \rightarrow 0_1^+$, and 1001.5-keV, $4_1^+ \rightarrow 2_1^+$, transitions of ^{122}Sn [10], and (d) the 1103.3- and 1030.3-keV transitions in Fig. 1. The energies of the transitions are in keV. Transitions associated with the complementary ^{95,96,97,98,100}Zr [21, 24–27] isotopes are indicated. Weak unlabelled peaks in both spectra are most likely contaminants.

FIG. 5: Background subtracted spectra from Experiment II gated on previously-known transitions belonging to ^{94,95,96}Zr [24, 27]. The energies of the transitions are in keV. The 1190.1- and 1237.8-keV transitions assigned to ^{118,120}Sn in the present work are indicated together with previously-known transitions of ^{116}Sn [32] (1293.6 keV), ^{117}Sn [28] (1278.2 keV), ^{118}Sn [7] (1229.7 keV), ^{119}Sn [29] (1220 keV), and ^{120}Sn [9] (1171.3 keV). The indicated 1194.4-keV transition is a previously-known transition of ^{94}Zr [24, 27]. Weak unlabelled peaks are most likely contaminants. The neutrons-emitted channels are also indicated for each combination of isotopes with respect to the ^{220}Th CN.

FIG. 6: (Color online) Examples of excitation functions for neutrons with energies up to 55 MeV deduced in Experiment IV for previously known transitions of ^{121}Sn [30] [the $(n, 4n)$ reaction channel], ^{122}Sn [10] [the $(n, 3n)$ reaction channel], and ^{123}Sn [31] [the $(n, 2n)$ reaction channel], as well as the 1103.3-keV transition (filled circles) assigned to ^{122}Sn in the present work. Specifically, the 1151-keV, $(15/2^-) \rightarrow 11/2^-$ transition (open triangles) of ^{121}Sn, the 1140.5-keV, $2^+ \rightarrow 0^+$ transition (open diamonds) of ^{122}Sn, and the 1107-keV, $(15/2^-) \rightarrow 11/2^-$ transition (open squares) of ^{123}Sn are shown. Lines connecting symbols are used to guide the eye.

FIG. 7: (Color online) Examples of excitation functions for neutrons with energies up to 75 MeV deduced in Experiment IV for previously known transitions of ^{119}Sn [29] [the $(n, 6n)$ reaction channel], ^{120}Sn [9] [the $(n, 5n)$ reaction channel], and ^{121}Sn [30] [the $(n, 4n)$ reaction channel], as well as the 1190.1-keV transition (filled circles) assigned to ^{120}Sn in the present work. Specifically, the 1220-keV, $(15/2^-) \rightarrow 11/2^-$ transition (open triangles) of ^{119}Sn, the 1171.3-keV, $2^+ \rightarrow 0^+$ transition (open diamonds) of ^{120}Sn, and the 1151-keV, $(15/2^-) \rightarrow 11/2^-$ transition (open squares) of ^{121}Sn are shown. Lines connecting symbols are used to guide the eye.

FIG. 8: (Color online) Examples of excitation functions for neutrons with energies up to 180 MeV deduced in Experiment IV for previously known transitions of ^{117}Sn [28] [the $(n, 8n)$ reaction channel], ^{118}Sn [7] [the $(n, 7n)$ reaction channel], and ^{119}Sn [29] [the $(n, 6n)$ reaction channel], as well as the 1237.8-keV transition (filled circles) assigned to ^{118}Sn in the present work. Specifically, the 1278.2-keV, $15/2^- \rightarrow 11/2^-$ transition (open triangles) of ^{117}Sn, the 1229.7-keV, $2^+ \rightarrow 0^+$ transition (open diamonds) of ^{118}Sn, and the 1220-keV, $(15/2^-) \rightarrow 11/2^-$ transition (open squares) of ^{119}Sn are shown. Lines connecting symbols are used to guide the eye.

FIG. 9: Systematics in the even-mass Sn isotopes from A=116 to A=130 of the 10_1^+ and 12_1^+ states. Data from Refs. [6–11, 32–35] and the present work. The excitation energy of the (12^+) state in ^{128}Sn is tentative [6].

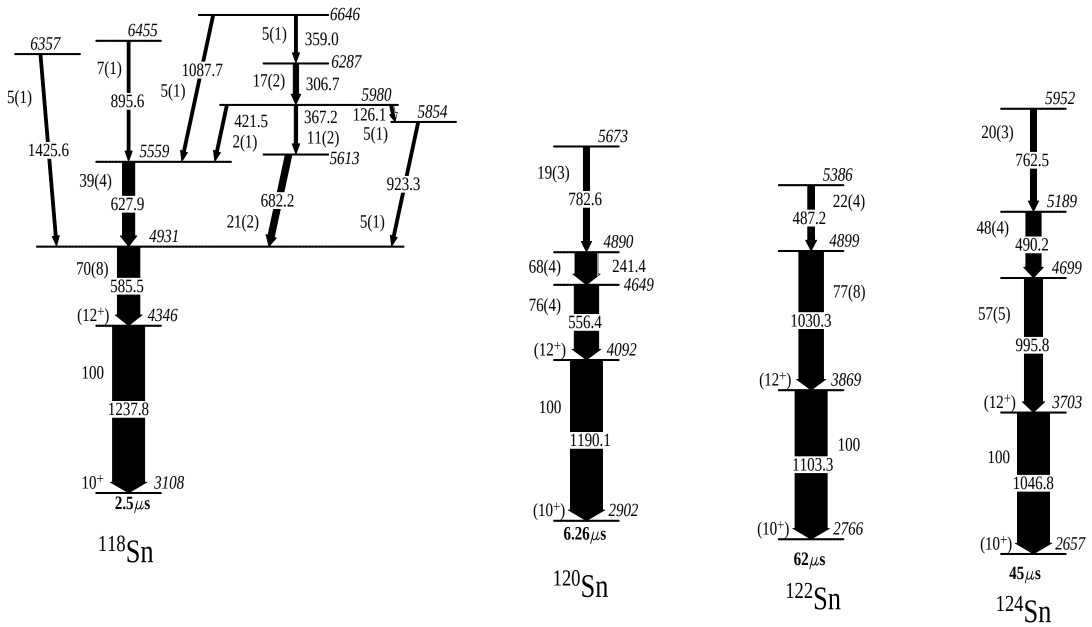

Figure 1 CK10248 24Oct2011

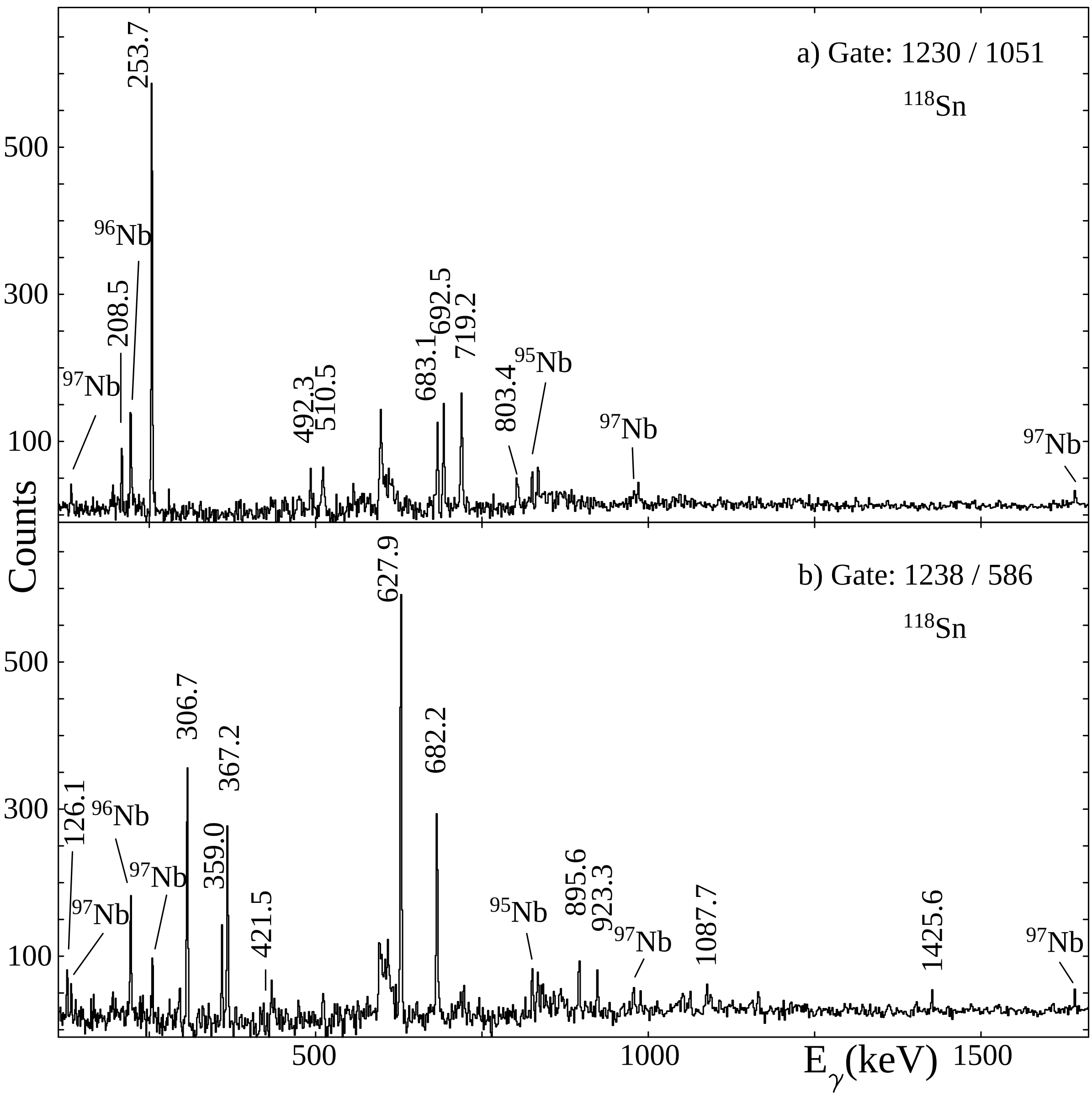

Figure 2 CK10248 24Oct2011

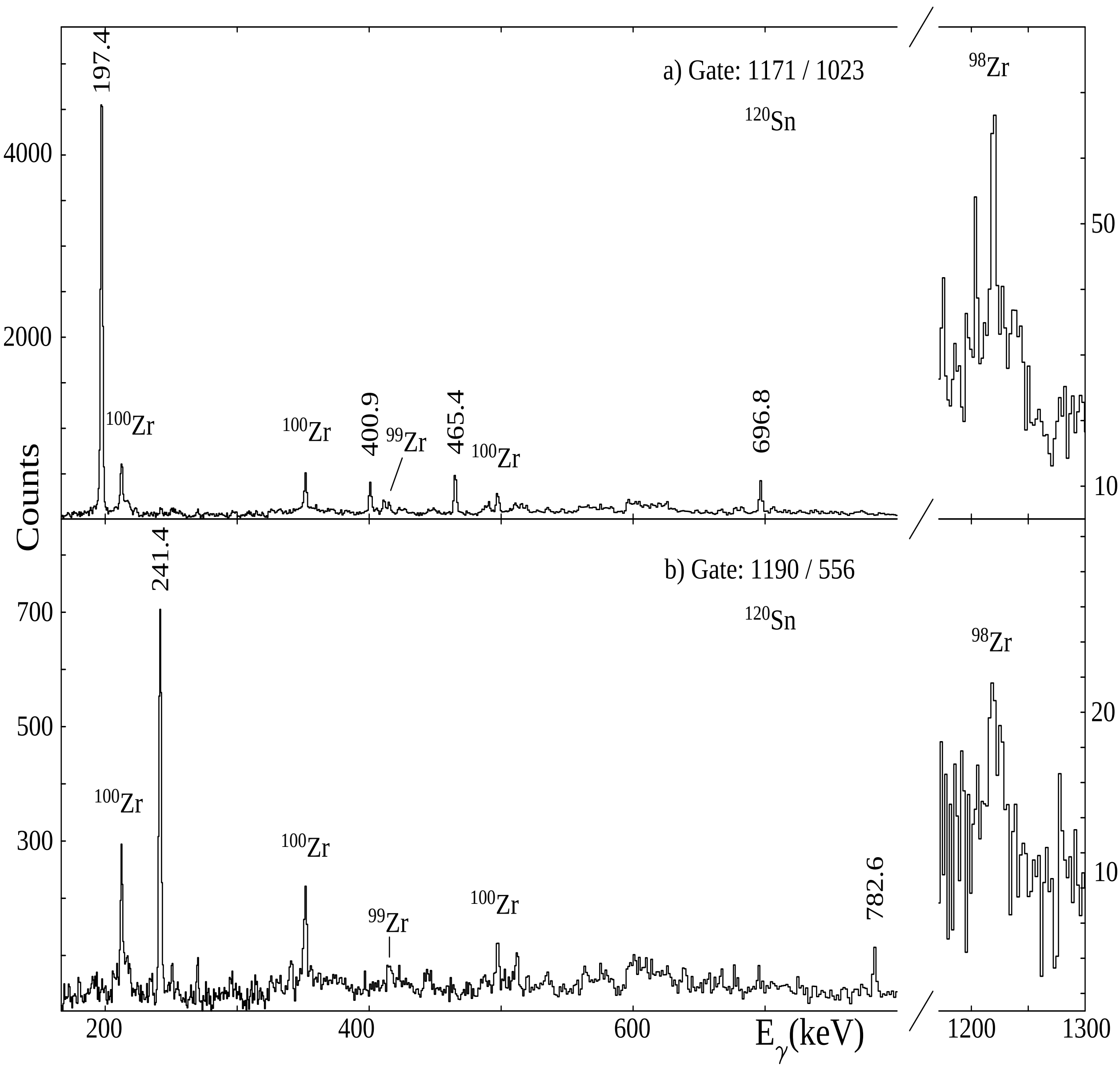

Figure 3 CK10248 24Oct2011

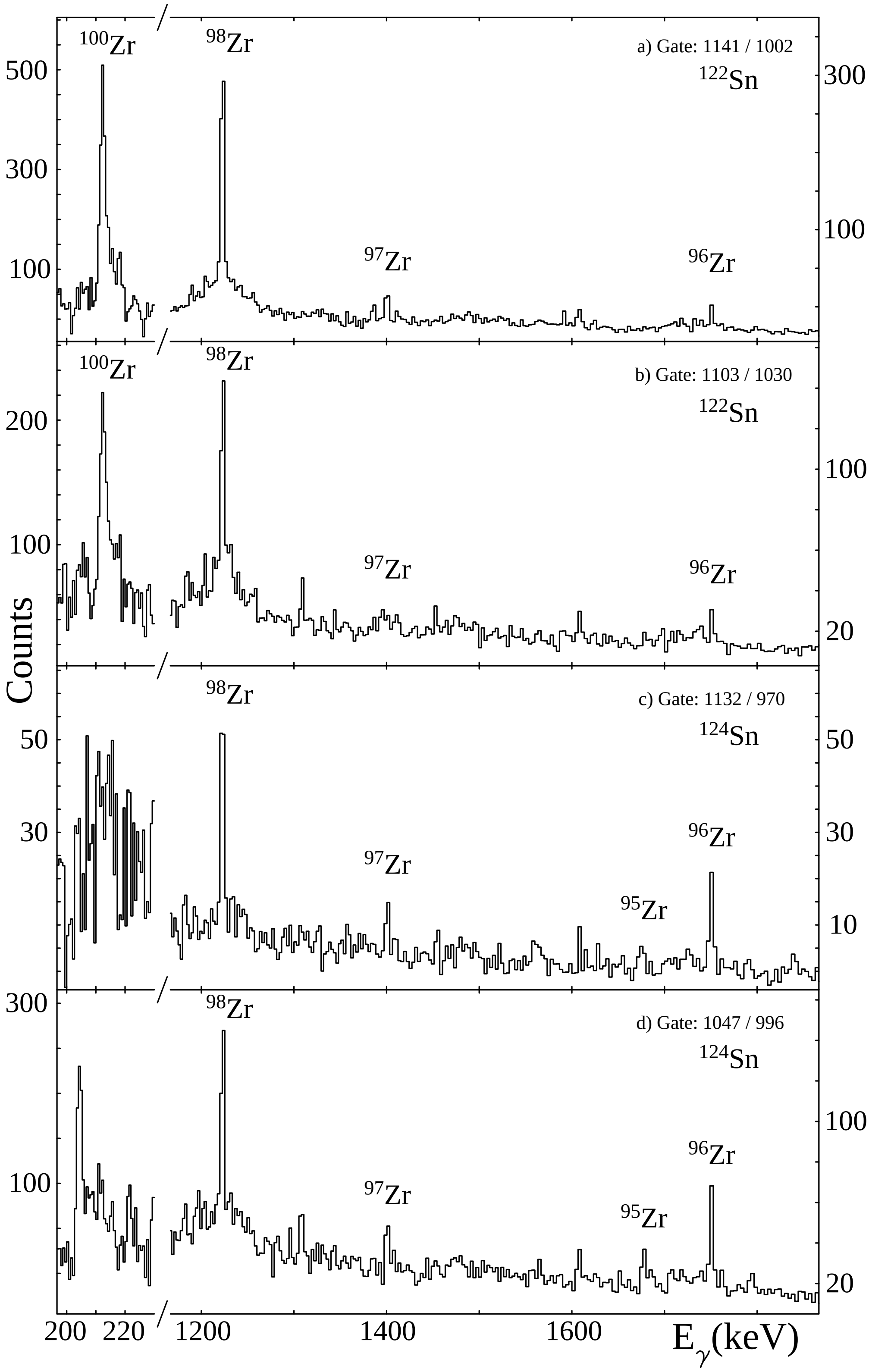

Figure 4 CK10248 24Oct2011

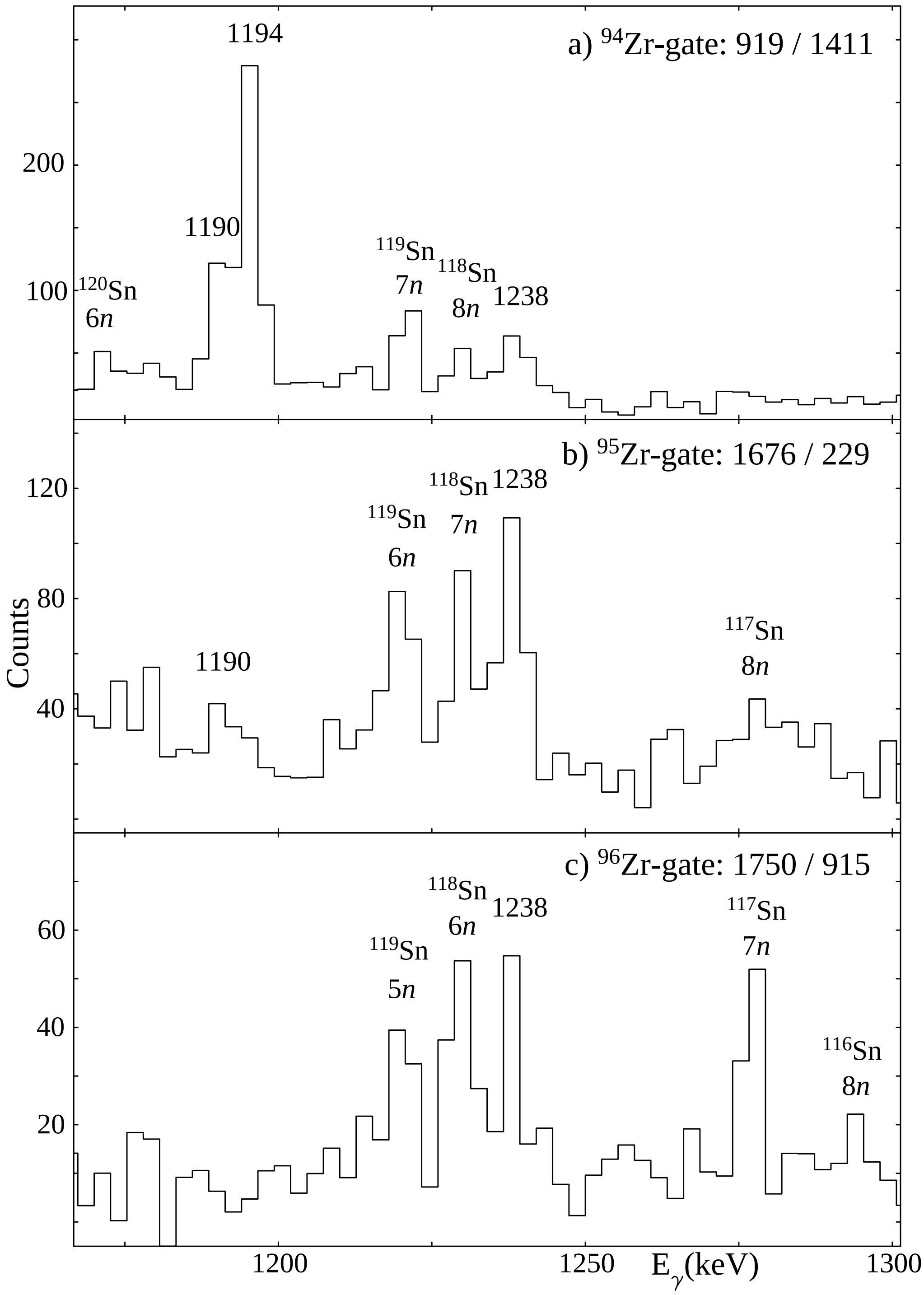

Figure 5 CK10248 24Oct2011

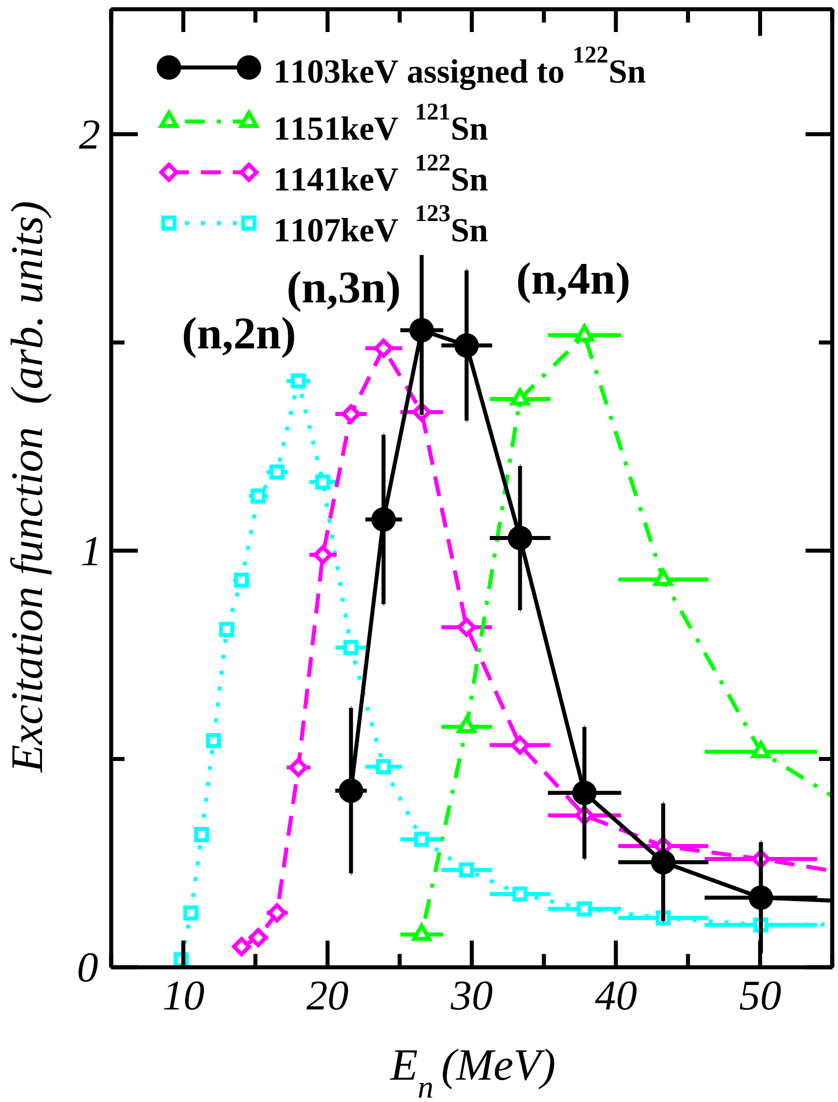

Figure 6 CK10248 24Oct2011

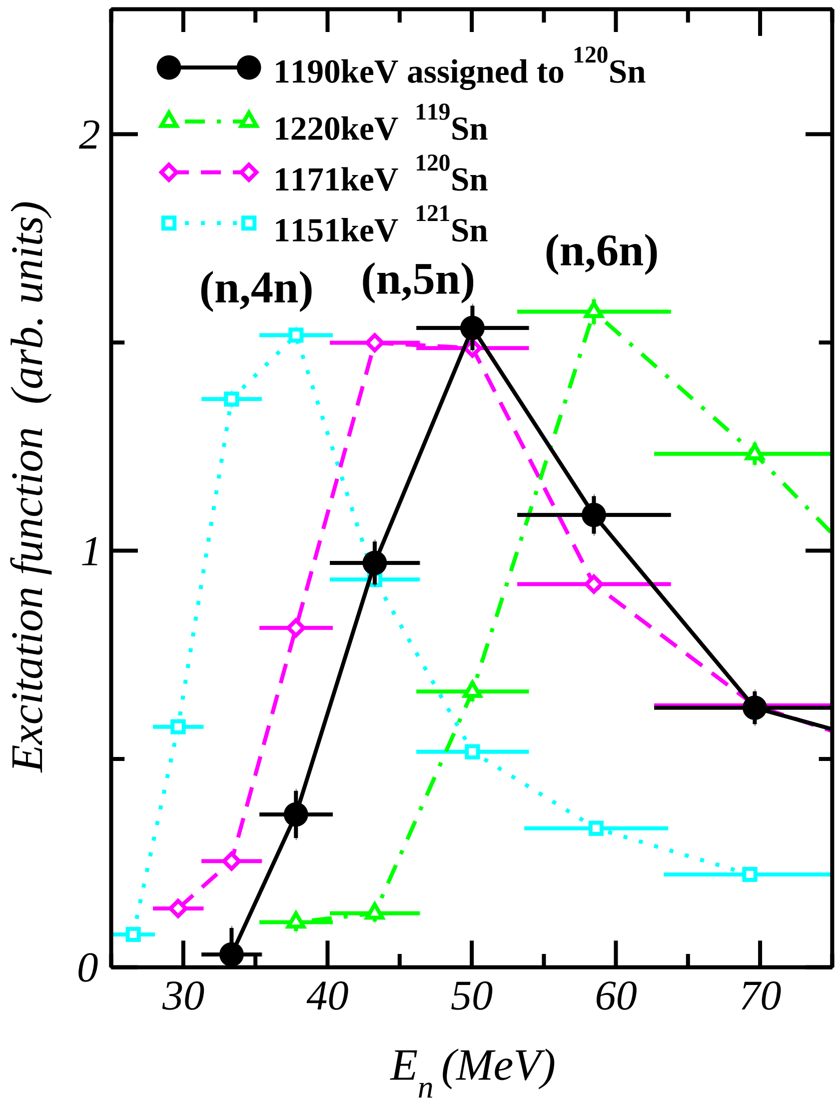

Figure 7 CK10248 24Oct2011

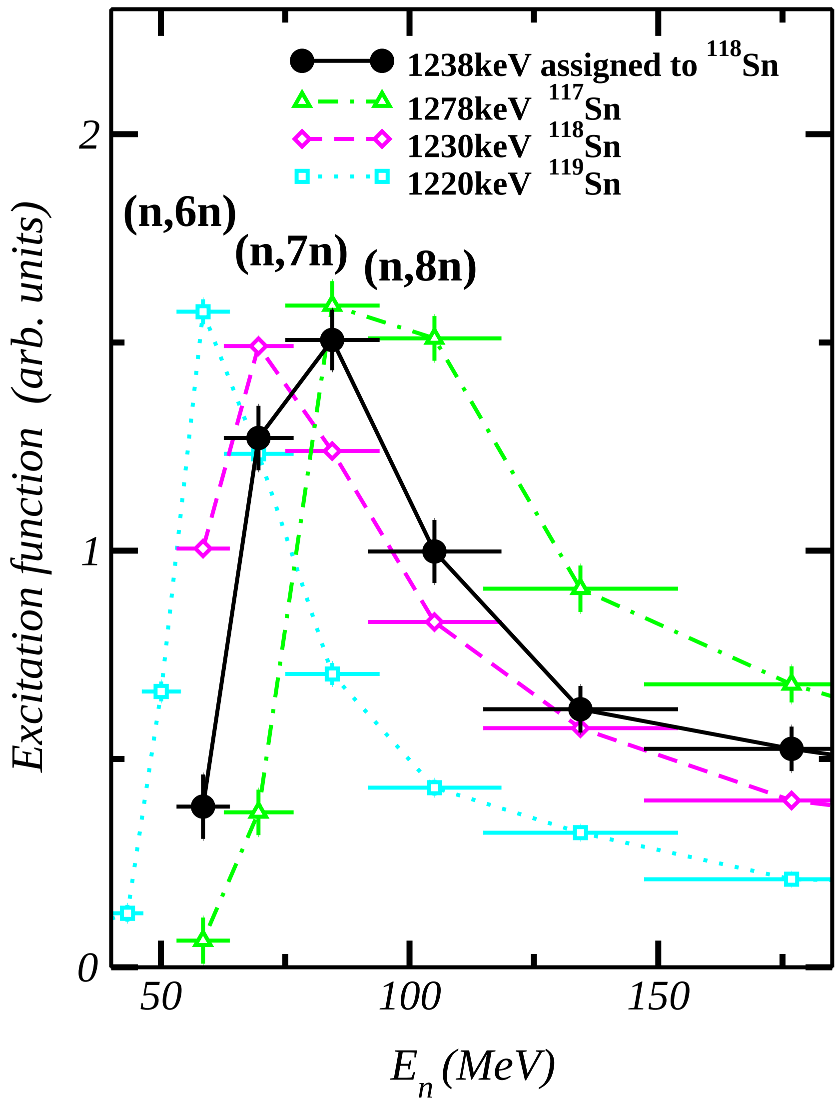

Figure 8 CK10248 24Oct2011

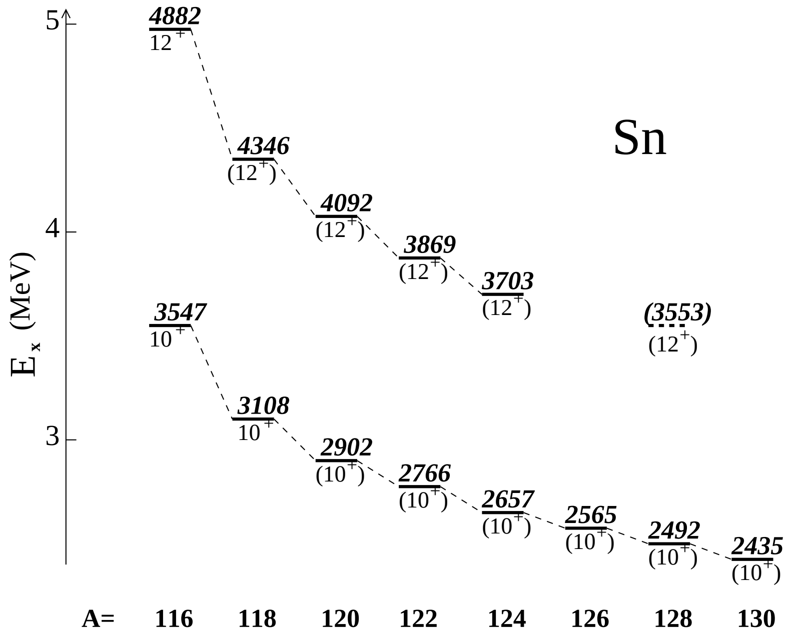

Figure 9 CK10248 24Oct2011